Biomedical Materials & Devices (2026) 4:638–654
https://doi.org/10.1007/s44174-025-00294-5

ORIGINAL ARTICLE

Biosynthesis of Cerium Oxide Nanoparticles Using *Alternanthera sessilis* Leaf Extract and Evaluation of their Antioxidant, Antibacterial, Anti-Inflammatory, Antidiabetic and Cytotoxic Activities

Manickam Rajkumar[1] · S. I. Davis Presley[1] · Prabha Govindaraj[2] · Krishnan Meenambigai[3] · Thandapani Gomathi[4] · Musab Mohammad Al-Essa[5] · Farid Menaa[6]

Received: 24 November 2024 / Accepted: 10 February 2025 / Published online: 4 March 2025

Abstract

Nanotechnology is a crucial field that is being widely researched in various fields. This innovative study investigates the synthesis of cerium oxide nanoparticles (CeO_2NPs) using an extract from the plant *Alternanthera sessilis* and its various biological applications. Several methods, such as UV–Vis spectroscopy, FTIR, XRD, FESEM, HR-TEM, and DLS analysis, were used to confirm the nature of the synthesized CeO_2NPs. In this study result, the UV–Vis spectroscopy maximum absorption peak at 326 nm proved that CeO_2NPs were present. FTIR analysis identified several functional groups, while XRD confirmed their crystal structure. It was seen in FESEM and HR-TEM images that CeO_2NPs were mostly spherical and oval, and their average size was 29 nm. CeO_2NPs exhibited impressive antioxidant properties and exhibited significant antibacterial activity against *E. coli* (25.04 ± 1.45 mm) and *S. aureus* (23.97 ± 1.29 mm). CeO_2NPs showed significant anti-inflammatory effects by inhibiting COX-1 ($80.91 \pm 1.22\%$) and COX-2 ($71.58 \pm 1.16\%$). CeO_2NPs showed strong enzyme-inhibitory activity against α-amylase ($70.46 \pm 1.37\%$), α-glucosidase ($79.58 \pm 1.37\%$), acetylcholinesterase ($68.92 \pm 1.39\%$), and butylcholinesterase ($73.47 \pm 1.53\%$). Cytotoxicity assays showed that CeO_2NPs significantly reduced cell viability by $28.59 \pm 0.39\%$ in HepG2 cancer cells. In conclusion, this study shows that the green-synthesized CeO_2NPs is a non-toxic, cost-effective and safe method, making it a very promising alternative for various biological applications.

Keywords Nanotechnology · *Alternanthera sessilis* · Antibacterial · Anti-Alzheimer's · Cytotoxicity

Introduction

Nanotechnology has the potential to transform various scientific fields. Nanomaterials provide a diverse array of applications due to their unique morphology and size, making them a prominent topic in both fundamental and applied sciences [1]. The development of various metal and metal-based nanoparticles has attracted significant research interest in recent years due to their unique properties in nanotechnology, including applications in biochemistry, bioimaging, catalysis, electrochemical and biomedicine [2–4]. Earlier research reports have shown that developing nanomaterials based on graphene and chitosan could be useful for making better biosensors and using them in a variety of biomedical applications [5–7]. Various methods, including environmentally friendly, chemical and physical techniques, can produce and stabilize metal-based nanoparticles. However, the chemical and physical methods frequently involve toxic substances, instability and necessitate multiple steps, as well

✉ S. I. Davis Presley
davispresleysi@ssn.edu.in

1 Department of Chemistry, Sri Sivasubramaniya Nadar College of Engineering, Chennai, Tamilnadu 603 110, India

2 Department of Chemistry, St. Joseph's Institute of Technology, Chennai, Tamil Nadu 636 119, India

3 Department of Pharmaceutical Engineering, Vinayaka Mission's Kirupananda Variyar Engineering College, Ariyanur, Salem, Tamil Nadu 636 308, India

4 PG and Research Department of Chemistry, D.K.M. College for Women (Autonomous), Vellore, Tamil Nadu 632 001, India

5 Pediatric Department, Faculty of Medicine, Al-Balqa Applied University (BAU), Salt 19117, Jordan

6 Department of Medicine and Nanomedicine, California Innovations Corporation (CIC), San Diego, CA 92037, USA

as high temperatures and pressures [8, 9]. These unsustainable metal nanoparticles are not suitable for medicinal applications such as drug delivery and treatments for diabetes and cancer. In contrast, the synthesis of metal nanoparticles using green technologies is innovative, cost-effective and takes place under mild reaction conditions [10, 11].

The green synthesis approach is a one-step method for producing nanoparticles (NPs) that require minimal energy for initiation and are non-toxic, biodegradable and cost-effective [12]. Additionally, it allows for the flexibility to create nanoparticles in various sizes, making it preferable to physical and chemical methods. Notably, NPs synthesized using plants as capping and bio-reducing agents exhibit enhanced stability and greater diversity in size and shape compared to those created with other materials [13]. This advantage is likely due to the rich genetic diversity of metabolites and biomolecules found in plants, including phenols, proteins, carbohydrates, vitamins and flavonoids [12, 14]. The functional groups of these plant metabolites, such as hydroxyl, carbonyl and amine, have been shown to reduce metal ions and decrease their size to the nanoscale [15]. Natural compounds present in biological systems play a crucial and diverse role in NPs synthesis, acting as capping and stabilizing agents. A review of the literature indicates that utilizing plants offers considerable advantages over other biosystems [16, 17]. Plants are easily accessible and convenient to work with, and the NPs they produce tend to be more stable. Consequently, various plant extracts synthesize nanoparticles using gold, silver, iron, copper and other metals [18, 19]. Previous studies have shown that nanomaterials are sensitive surface plasmon sensor methods that have many biomedical applications [20–22]. However, due to their diverse properties, their applications in medical fields have proven to be very limited.

Cerium oxide nanoparticles (CeO_2NPs) have been identified as biosafe, non-toxic and biocompatible, making them suitable for a range of biological and environmental applications [23]. Because they are antifungal, antibacterial, wound-healing, anti-inflammatory, anti-diabetic, anticancer and antioxidant, CeO_2NPs have a lot of potential in drug delivery, biolabeling, biological properties and nanomedicine [24]. Recent research has shown that CeO_2NPs effectively inhibit a wide range of microorganisms, including bacteria, fungi, viruses and certain pathogens [25]. Numerous studies have been published detailing the synthesis of metal nanoparticles using various plant-based materials, including flowers, leaves, roots, stems, bark, fruit, buds and latex, as part of green approaches for fabricating CeO_2NPs [26, 27]. Recent publications indicate that many investigations have focused on understanding the role of the phytochemicals involved in the green synthesis and stability of CeO_2NPs through phyto-based materials. Consequently, researchers have documented the biofabrication of CeO_2NPs using various plant species such as *Origanum majorana* [28], *Ceratonia siliqua* [29], *Oroxylum indicum* [30] and *Carica papaya* [31]. Therefore, the aforementioned literature confirms that CeO_2NPs are excellent inorganic nanomaterials for applications in drug delivery, the food industry, pharmaceuticals and biological uses [32].

Alternanthera sessilis (*A. sessilis*) is a perennial herb that typically grows to a height of 30–60 cm and is a traditional medicinal value plant [33]. Typically found in tropical and subtropical regions, this plant can thrive in a variety of environmental conditions. People have traditionally used herbal medicine to treat various ailments like digestive issues, inflammation and skin conditions [34]. The *A. sessilis* plant has a higher level of antioxidant activity, antimicrobial properties, anticancer potential, wound healing and hepatoprotective activities [35]. The plant is rich in bioactive compounds, including flavonoids, phenolic acids and vitamins, contributing to its antioxidant and anti-inflammatory properties. *A. sessilis* is notable for its potential in the green synthesis of nanoparticles, such as silver and zinc oxide nanoparticles, which have various applications in pharmaceuticals, biomedical fields and agriculture [35, 36]. Although most of the biomedical properties have been investigated through pharmacological knowledge, phytochemical studies of this plant have only demonstrated a specific and limited potential application in nanotechnology. These plant-based biological applications require thorough exploration. However, there are very few references about NPs from this plant. Moreover, no study has yet demonstrated the synthesis of CeO-NPs from *A. sessilis* plant and its biological applications.

The novelty of this study is that CeO_2NPs were synthesized using a simple and cost-effective extract of *Alternanthera sessilis* in accordance with the principles of green chemistry. The morphological features and physical properties of the synthesized CeO_2NPs were evaluated using characterization techniques such as UV–Vis absorption spectroscopy, FTIR, XRD, FESEM, HR-TEM and DLS analysis. The synthesized CeO_2NPs were evaluated for their various biological applications such as antioxidant, antibacterial, anti-inflammatory, anti-diabetic, anti-cholinergic and cytotoxic activities (Scheme 1).

Experimental

Materials

Cerium(III) nitrate hexahydrate, sodium hydroxide (NaOH), Ethylenediaminetetraacetic acid (EDTA), trichloroacetic acid (TCA), Cyclooxygenase (COX-1 Inhibitor, FR122047 and COX-2 Inhibitor V, FK3311), p-Nitrophenyl-α-D-glucopyranoside (P-NPG), 5,5′-Dithio-bis-(2-nitrobenzoic Acid) (DTNB), Dulbecco's Modified Eagle's Medium

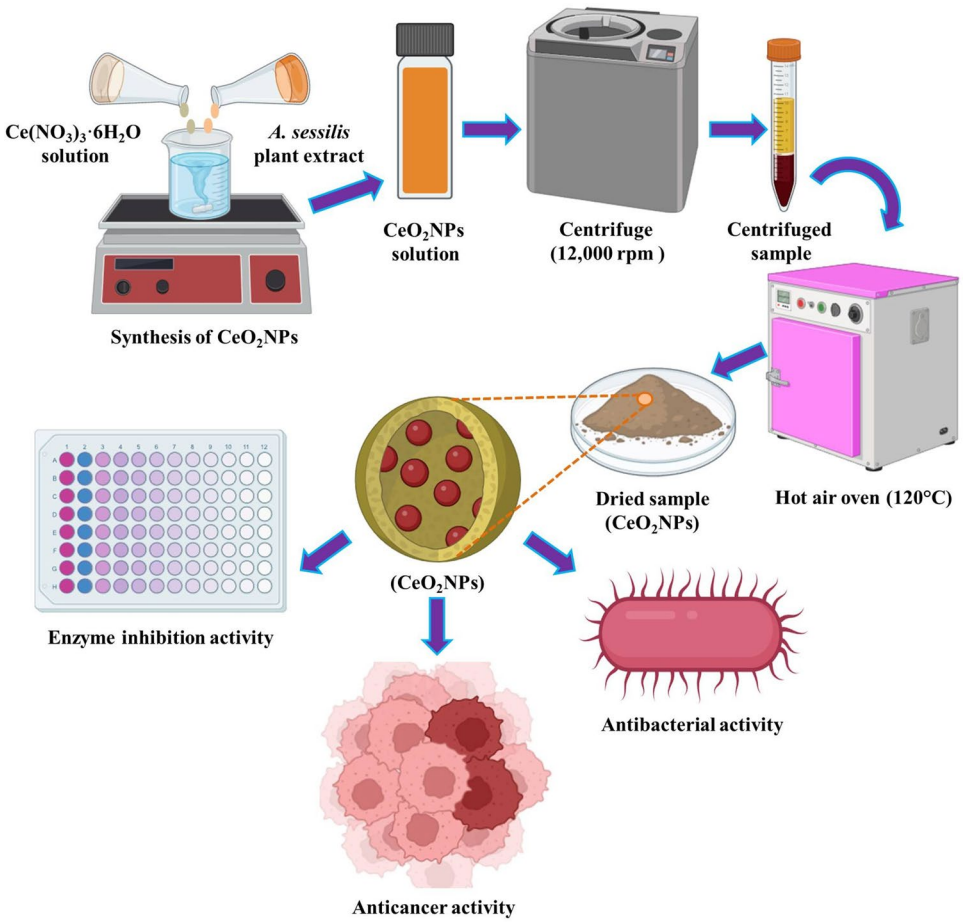

Scheme 1 Synthesis of CeO_2NPs using *A. sessilis* plant extract and their various biological applications is depicted schematically

(DMEM), 3-(4, 5-dimethylthiazol-2-yl)-2, 5-diphenyl tetrazolium bromide (MTT) and dimethyl sulfoxide (DMSO) was purchased from Sigma Aldrich, India.

Preparation of Plant Extract

From the botanical garden at SSN College of Engineering in Chennai, Tamil Nadu, India, fresh *Alternanthera sessilis* plant leaves were collected. Following a thorough washing with distilled water, the leaves were left to dry at room temperature away from the sunlight. Next, the leaves were finely ground into powder. Then, 10 g of this plant powder was added to 100 mL of distilled water and stirred continuously at 60 °C for 2 h using magnetic stirring. Then, the solution was filtered thoroughly through Whatman No. 1 filter paper. The plant extract was collected and stored in a freezer at 4 °C for future use [37].

Synthesis of CeO_2NPs

The CeO_2NPs were synthesized using a previously described method with minor modifications [28, 30]. A 0.5 M solution of cerium nitrate hexahydrate ($Ce(NO_3)_3{\cdot}6H_2O$) was made in deionized water. 10 mL of a precursor solution made from *Alternanthera sessilis* leaf extract was then added. Next, add a 2 M NaOH solution drop wise to the mixture. The resulting solution was then centrifuged at 12,000 rpm for 20 min, washed with distilled water three times and followed by ethanol. The obtained precipitates were dried at 80 °C for 6 h and subsequently dried at 120 °C for 4 h. Finally, a fine powder containing CeO_2NPs mediated by *A. sessilis* extract was obtained and stored for further studies.

Characterization of CeO_2NPs

A variety of techniques were employed to characterize the synthesized CeO_2NPs. The optical properties of the nanoparticles are measured using a UV–Vis spectrophotometer (Shimadzu UV-1800) across a wavelength range of 200 to 800 nm. FTIR analysis (Model AIM-8800, spectral range of 4000–400 cm^{-1}) was conducted to identify the phytochemical components that require reduction and capping by metal ions. The phase purity and crystalline structure were examined using a powder XRD diffractometer (Shimadzu-7000), utilizing Cu Kα radiation ($\lambda = 1.541$ Å) at a voltage of 50 kV and a current of 30 mA, with 2θ values ranging from 10° to

80°. Surface morphology and compositional analysis was performed using FESEM (Carl Zeiss FESEM at 10 kV) equipped with an EDS system and transmission electron microscopy (HRTEM, Thermo fisher). Additionally, analyzed the average zeta potential and particle size distribution of the CeO_2NPs using DLS (Malvern Zetasizer, Nano-S90, UK).

Antioxidant Activity

DPPH (2, 2-diphenyl-1-picryl-hydrazyl-hydrate) Assay

The DPPH free-radical scavenging activity of CeO_2NPs was evaluated using the previous method [38]. Briefly, a 0.2 mM DPPH solution was prepared in methanol, and varying concentrations of CeO_2NPs (10, 50, 100, 150 and 200 µg/mL) were also dissolved in methanol. 50 µL of the DPPH solution was added to micro plates with different amounts of nanoparticles. After shaking the reaction mixture, incubate it in the dark for 30 min. After measuring the absorbance at 570 nm, the scavenging activity was computed using the formula below:

$$\text{Inhibition (\%)} = \left[\frac{\text{Absorbance (Control)} - \text{Absorbance(Sample)}}{\text{Absorbance (Control)}}\right] \text{x } 100 \quad (1)$$

ABTS (2, 2'-azino-bis(3-ethylbenzothiazoline-6-sulfonic acid)) Assay

An 8 mM stock solution was prepared by dissolving 44 mg of ABTS in 10 mL of distilled water [38]. Equal volumes of a 3 mM potassium persulfate solution were added to generate the ABTS radical cation ($ABTS^{\bullet+}$). Then incubated this mixture in the dark at 25 °C for 12 to 18 h. Before the experiment, prepared a fresh working solution of ABTS radical by mixing $ABTS^{\bullet+}$ with methanol in a 1:2 ratio. It was mixed with 290 µL of the ABTS radical solution in a 96-well plate. The test sample solution had concentrations of 10, 50, 100, 150 and 200 µg/mL. The mixture was allowed to sit for 30 min at 25 °C, after which the absorbance was measured at 734 nm using a Microplate Reader (BioTek, ELX800) and calculated using Eq. (1).

Hydrogen Peroxide (H_2O_2) Scavenging Assay

The previous method was used to examine the effect of CeO_2NPs on the scavenging of hydrogen peroxide [39]. A 40 mM solution of hydrogen peroxide was prepared using phosphate buffer saline (PBS). Next, treat different concentrations (10, 50, 100, 150 and 200 µg/mL) of CeO_2NPs with 0.6 mL of the 40 mM H_2O_2 solution and incubate for 10 min before measuring the absorbance at 230 nm and and calculated using Eq. (1).

Superoxide Dismutase (SOD) Activity

CeO_2NPs capacity to scavenge superoxide radicals was assessed using a solution that contained 0.02 mM riboflavin, 50 mM PBS, and 1 mM EDTA [40]. Nitroblue tetrazolium at a concentration of 0.75 mM was added to the mixture. Next, treat the reaction with CeO_2NPs at various concentrations of 10, 50, 100, 150 and 200 µg/mL. After exposure to fluorescent light for 7 min, the scavenging activity was measured at 560 nm and and calculated using Eq. (1).

Reducing Power Activity

Different concentrations of CeO_2NPs (10, 50, 100, 150 and 200 µg/mL) with 200 mM sodium phosphate buffer and ferricyanide were used to assess their reducing power potential [41]. Next, incubate the mixture in the dark at 50 °C for 20 min. The reaction was subsequently stopped by adding 50 µL of TCA. The reaction sample was centrifuged for 10 min at 3000 rpm in order to extract the supernatant. A volume of 50 µL of the supernatant was added to microtiter plates containing 0.1% ferric chloride, and the plates were incubated for 10 min. Then, the absorbance limit was measured at 700 nm and calculated.

FRAP (Ferric reducing antioxidant power) Assay

A FRAP assay was performed following the previously established protocol [42]. To 0.2 M sodium phosphate (1 mL), 1% potassium ferricyanide (1 mL) was added. This mixture was then combined with 1 mL of CeO_2NPs at varying concentrations (10, 50, 100, 150 and 200 µg/mL) and incubated for 20 min at 50 °C. After adding 2.5 mL of 10% TCA, the mixture was centrifuged at 3000 rpm for 10 min. After this, mix the supernatant (1.5 mL) with distilled water (1.5 mL), 0.1% $FeCl_3$, and 0.1 mL of the appropriate reagent. The absorbance was then measured at 700 nm and calculated using Eq. (1).

Antibacterial Activity

The antibacterial potential of CeO_2NPs was evaluated against *Staphylococcus aureus, Bacillus subtilis, Escherichia coli, Klebsiella pneumonia,* and *Salmonella typhi* using the Kirby-Bauer disk diffusion method [43]. Microbial strains were subcultured in nutrient broth overnight at 37 °C. Following this, 100 µL (1×10^6 cfu/mL) of the

overnight cultures were inoculated into the sterilized nutrient broth and incubated at 37 °C for 4–5 h. Mueller–Hinton agar (20 mL) was applied to petri plates and left to harden. Next, 100 µL of the microbial inocula (1×10^6 cfu/mL) was evenly spread onto the agar surface. After the 6 mm filter paper discs were autoclaved and filled with 10, 50, 100, 150 and 200µL of synthesized CeO_2NPs, they were put on the agar plates and left to grow overnight at 37 °C. The zones of bacterial growth inhibition around the discs were measured. This assay was conducted in triplicate and the zone of inhibition values were measured. Streptomycin served as the standard control.

Anti-Inflammatory Activity

Following the procedure described by Tanaka et al. [44], the inhibitory properties of CeO_2NPs on COX were evaluated using the COX-1 and COX-2 test kits. The substrate was 1.1 mM arachidonic acid, while the positive control was a 10 mM Ibuprofen solution. Evaluated the ability of CeO_2NPs to inhibit the peroxidase activity of COXs according to the kit manufacture instructions. Absorbance at 590 nm was measured and calculated using the Synergy II reader (BioTek Instruments, USA) to colorimetrically detect N,N,N',N'-tetramethyl-p-phenylenediamine in 96-well plates.

Antidiabetic Activity

α-Amylase Inhibition Activity

The α-amylase inhibitory assay was performed according to the previous method with minor modifications [45]. The reaction took place in a 96-well microplate using an assay mixture consisting of 50 µL of 50 mM PBS, 50 µL of 16 U/mg α-amylase and varying concentrations of CeO_2NPs (10–200 µg/mL) at a pH of 5.8, which was pre-incubated at room temperature for 15 min. Then, 50 µL of 1% soluble starch (50 mM PBS) was added as a substrate to start the reaction. It was left to sit at room temperature for incubation for 10 min. After incubation, the absorbance of the reaction mixture at 405 nm was measured spectrophotometrically. The inhibition of α-amylase activity was expressed as a percentage of inhibitory activity using the following formula in comparison to the standard drug Acarbose.

$$\alpha - \text{amylase inhibition } (\%) = \left[\frac{\text{Absorbance (Control)} - \text{Absorbance(Sample)}}{\text{Absorbance (Control)}}\right] \text{x } 100$$

α-Glucosidase Inhibition Activity

The analysis of α-glucosidase inhibition activity was conducted following the previous method [45]. Briefly, a 96-well microplate was pre-mixed with 50 µL of 0.3 mM PBS at pH 6.8, 40 µL of α-glucosidase (1 U/mL) and 20 µL of different doses of CeO_2NPs (10–200 µg/mL) and incubated at 37 °C for 10 min. After that, 40 µL of 2 mM P-NPG was added and the reaction was left to continue for another 10 min at 37 °C. The reaction was then terminated by adding 70 µL of Na_2CO_3 (0.2 M). A microplate reader was used to measure the p-nitrophenol release spectrophotometrically at 405 nm and the results were compared to those of the reference medication acarbose. The α-glucosidase inhibitory activity was determined using the following formula:

$$\alpha - \text{glucosidase inhibition } (\%) = \left[\frac{\text{Absorbance (Control)} - \text{Absorbance(Sample)}}{\text{Absorbance (Control)}}\right] \text{x } 100$$

Cholinesterase (ChE) Inhibition Activity

The inhibition of acetylcholinesterase (AChE) and butylcholinesterase (BChE) was evaluated using Ellman's method with slight modifications [46]. A sample of CeO_2NPs and the standard galantamine was prepared in 1 mL of DMSO along with appropriate amounts of PBS (pH 7.7) at varying concentrations. Some test samples (25 µL), DTNB in buffer (80 µL) and an enzyme (AChE/BChE, 2 U/mL) were put in a 96-well plate and left there for 5 min. Following this, 15 µL of the substrate (acetylthiocholine iodide and butyrilthiocholine iodide) was added and the mixture was incubated for an additional 5 min. The absorbance was then measured with a micro plate reader at 415 nm and 25 °C. The percentage of inhibition was calculated using the following equation:

$$\text{Enzyme inhibition activity } (\%) = 1 - \left[\frac{\text{Absorbance (Sample)}}{\text{Absorbance (Control)}}\right] \text{x } 100$$

Cytotoxicity Assay

Human lung adenocarcinoma cells (HepG2) were obtained from the National Centre for Cell Sciences (NCCS) in Pune, India. DMEM was used to cultivate these cells. An antibiotic solution containing 100 U/mL of penicillin and 100 µg/mL of streptomycin was also added, along with 10% fetal bovine serum. The cells were subculture until they achieved 70% confluence after being incubated at 37 °C with 5% CO_2.

The cytotoxicity of CeO_2NPs on HepG2 cells was assessed using the MTT assay [47]. A stock solution of the test sample was prepared by dispersing CeO_2NPs (10 mg/mL) in a culture medium and sonicating for 1 h to prevent particle agglomeration. From the stock solution, different amounts of CeO_2NPs (12.5, 25, 50, 100 and 200 µg/

mL) were taken and vortexed vigorously for 30 s before the experiment. A layer of cells that were completely connected was trypsinized and seeded into 96-well tissue culture plates at a density of 5×10^3 cells/well. The plates were then kept at 37 °C with 5% CO_2 for 24 h. Different concentrations of the test samples were added to the cells and incubated for an additional 48 h in the same conditions. After that, 100 µL of MTT solution (1 mg/mL) was put into each well. The plates were then left to sit for 4 h so that formazan crystals could form. The used media was taken out after incubation and 100 µL of DMSO was added to break up the formazan crystals. A microplate reader was used to measure the absorbance at 570 nm. The viability of the cells was calculated using the following formula:

$$\text{Cell viability (\%)} = \left[\frac{\text{Number of live cells} - \text{dead cells}}{\text{Total number of cells}}\right] \text{x } 100$$

Statistical Analysis

Each experiment was conducted in triplicates (n = 3) and the data are expressed as mean ± SD. A comparative analysis of the differences between control and experimental values was performed using one-way analysis of variance (ANOVA) by Graph Pad Prism version 10.2.3 software. Statistical significance was noted for p values less than 0.05 ($p < 0.05$).

Results and Discussion

UV–Visible Spectral Analysis

The UV–Vis spectroscopy analysis revealed that CeO_2NPs display distinct absorption peaks in the UV region. The CeO_2NPs exhibited sharp absorption maxima at 323 nm, 326 nm and 332 nm across different concentrations (Fig. 1). The 300–340 nm peaks are caused by CeO_2NPs intrinsic band-gap absorption, which is caused by electronic transitions between the valence and conduction bands [48]. The absorption spectra provide insights into the nanoparticles' physical properties, including size, shape and synthesis conditions. The strong, narrow absorption peaks in the UV region suggest these nanoparticles' potential for medical and industrial applications [49]. These results are similar to those from earlier research that used *Salvadora persica* aqueous extract to make CeO_2NPs and found similar absorption peaks in the 320–330 nm [27].

FTIR Analysis

FT-IR analysis helps to identify the various functional groups attached to the surface of CeO_2NPs. Figure 2 displays the FTIR spectrum result of CeO_2NPs synthesized

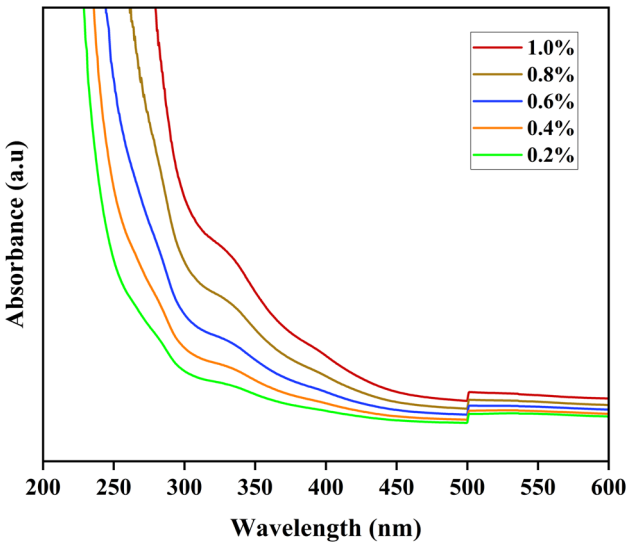

Fig. 1 UV–Vis absorption spectral analysis of synthesized CeO_2NPs at different concentrations

using *A. sessilis* extract. The FTIR analysis results of CeO_2NPs synthesized from plant extracts showed the presence of various major functional groups by scanning in the wavelength range of 400 to 4000 cm^{-1}. In particular, the synthesized CeO_2NPs show clear resonance peaks at wavenumbers 3448, 1645, 1567, 1388, 1078, 658, and 564 cm^{-1}. The vibrational peaks at 564 and 658 cm^{-1} are due to Ce–O stretching and the absorption band at 1567 and 1388 indicates the presence of C–O bonds. FTIR analysis of CeO_2NPs indicated that the peaks recorded at 3448 cm^{-1} indicate the presence of O–H groups, while the vibrational stretches at 1645 cm^{-1} are due to and due

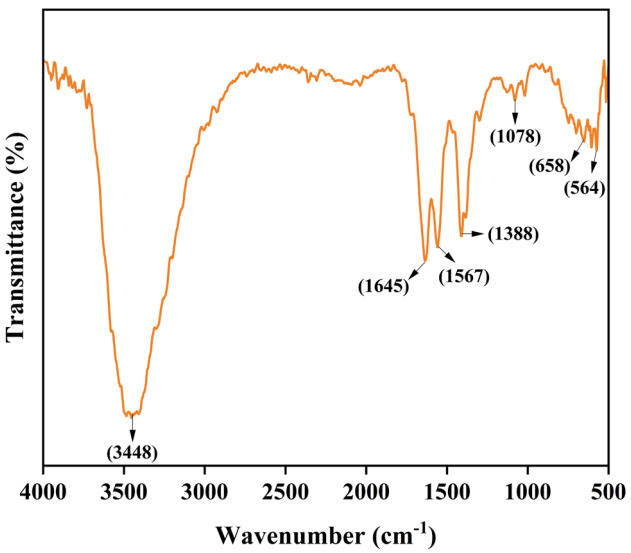

Fig. 2 FTIR spectral analysis of synthesized CeO_2NPs

to the presence of C–H group. The increased volumes of CeO_2NPs showed all the characteristic peaks and matched the individual vibrational stretches of CeO with little change in peak stability. The CeO_2NPs spectrum had similar absorption patterns to the extract, but they were less intense and had slightly lower frequencies [50]. This implies that the plant's biomolecules encircled the nanoparticles during their formation. This confirms that biological molecules play a crucial role in the green synthesis and stabilization of CeO_2NPs in aqueous media [27]. The characteristic peaks at 658 and 564 cm^{-1} particularly confirm the successful formation of CeO_2NPs [51].

XRD Analysis

The material identity, crystallinity, size, and purity of the green-synthesized CeO_2NPs were determined by analyzing the X-ray diffraction patterns. As shown in Fig. 3, the spectral analysis of the NPs showed that the most stable edge peaks were observed, demonstrating the crystallinity of the CeO_2NPs. The biosynthesized CeO_2NPs showed clear diffraction peaks at 2θ values of 28.6°, 33.1°, 47.5°, 56.4°, 59.1°, 68.1°, 76.8° and 79.1°. Furthermore, these peaks corresponded to the (111), (200), (220), (311), (222), (400), (331) and (420) crystallographic planes. There were no impurity peaks found in the patterns, and all of the peaks closely matched the standard CeO_2NPs (JCPDS PDF: 34–0394) pattern, which is the face-centered cubic (FCC) structure. This structure matches what was seen when similar XRD results were found in a previous study for CeO_2NPs made from *Olea europaea* leaf extract [52]. The absence of additional peaks in the XRD pattern indicates excellent purity of the produced nanoparticles. These results are consistent with previous research that found the presence of major crystallographic sites as XRD peaks in CeO_2NPs prepared from oysters [51].

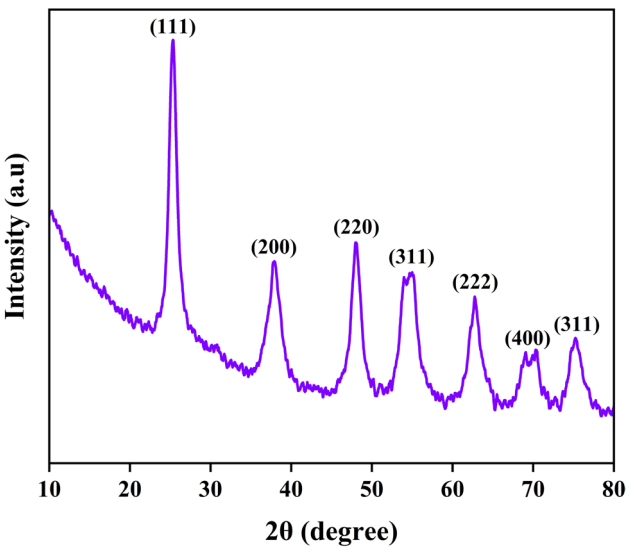

Fig. 3 XRD pattern analysis of synthesized CeO_2NPs

FESEM and HR-TEM Analysis

The electron microscopic technique serves as a robust tool for assessing the size and shape of synthesized nanoparticles. Figure 4 illustrates the FESEM and HR-TEM images of the biosynthesized CeO_2NPs. The FESEM analysis shows that the synthesized CeO_2 NPs are evenly spread out and mostly spherical and oval in shape (Fig. 4A). Further analysis using HR-TEM shows that the final product is made up of closely packed nanoparticles that are 28–32 nm across and oval in shape (Fig. 4B). The particle size distribution histogram from the HR-TEM micrograph analysis shows that the particles are mostly the same size, with a median diameter of 29.7 ± 0.5 nm. The CeO_2NPs made from *Origanum majorana* plant extracts also have a spherical shape, measuring between 10 and 70 nm and this is mostly because of the flavonoids and phenolic compounds found in the plant extract [28]. Additionally, another study found that the synthesized CeO_2NPs exhibited spherical shapes with an average particle size of 15 nm [51].

DLS and Zeta Potential Analysis

The DLS technology is used to look at the sample's particle size distribution. It treats each particle as a separate sphere moving in Brownian motion and given a hydrodynamic radius. DLS is mainly used to determine the particle size and shell thickness of a capping or stabilizing agent that forms metal nanoparticles. DLS primarily determines the particle size and shell thickness of capping or stabilizing agents, which helps in the growth of synthesized nanoparticles [53]. As shown in Fig. 5A, the synthesized CeO_2NPs show a narrow particle size distribution and their average particle size is calculated to be 94 nm.

Zeta energy (ZP) values reveal details regarding the surface area charge and stability of the samples. Figure 5B shows that CeO_2NPs have an average ZP value of − 28.57 mV. The ZP value of − 28.57 mV clearly indicates that the biocompatible CeO_2NPs have excellent stability. The high negative values of zeta energy confirm that the closed particles on the surface of CeO_2NPs mainly contain negatively charged groups, which have stability of the nanoparticles. Proteins in *A. sessilis* leaf extract are responsible for the reduction of metal ions. They are efficient in stabilizing the aggregated nanoparticles. Previous research reported that green-synthesized CeO_2NPs exhibited size of 45 nm, along with a negative charge [54].

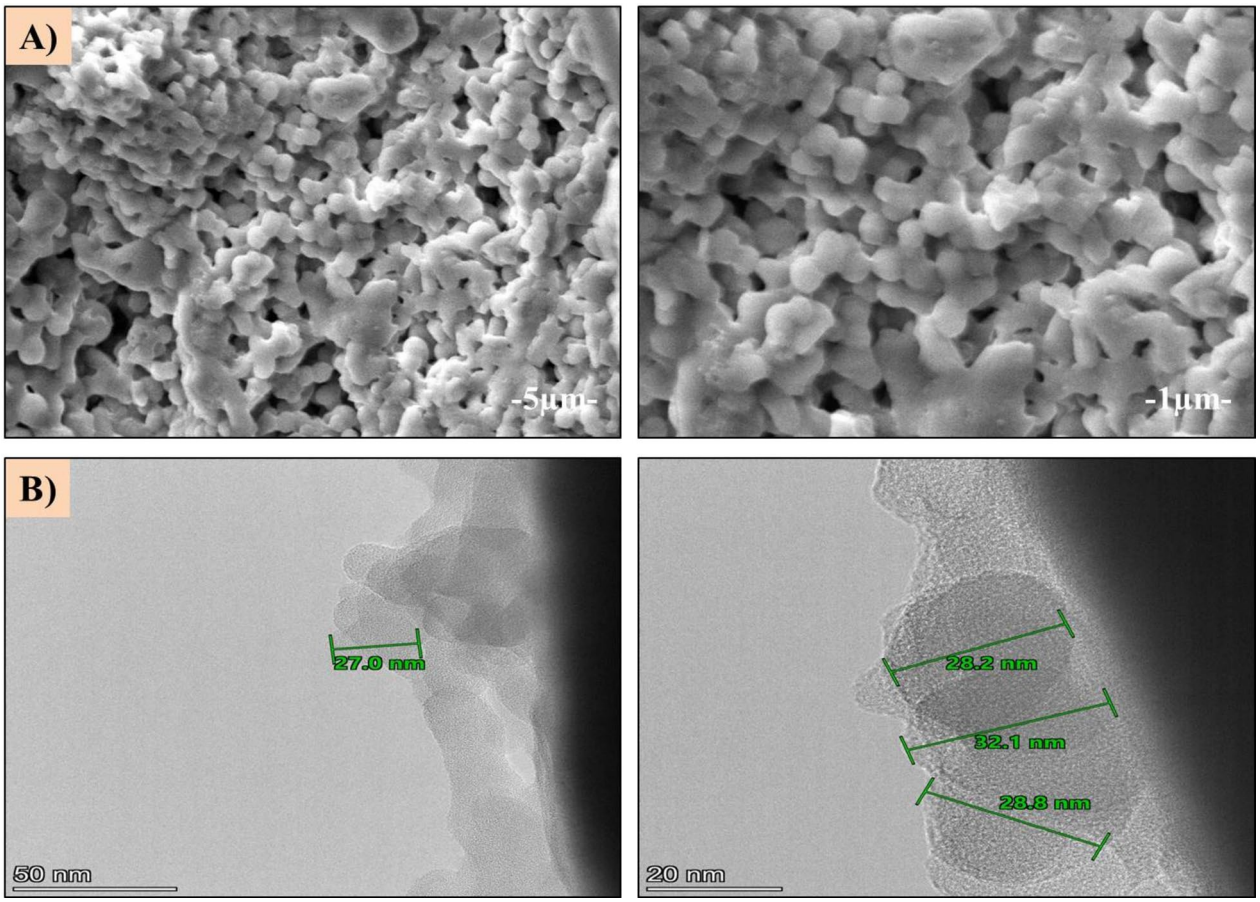

Fig. 4 **A** FESEM and (**B**) HR-TEM morphology analysis of synthesized CeO_2NPs

Antioxidant Activity

Antioxidants are substances that can neutralize reactive species by inhibiting oxidation reactions, thereby shielding cells from damage resulting from the overproduction of reactive oxygen species (ROS) [55]. Numerous natural compounds found in plant extracts have antioxidant properties. The demand for these natural antioxidants is high due to their effectiveness in mitigating ROS-related pathogenesis associated with various degenerative diseases [56]. To assess the antioxidant capacity of biosynthesized CeO_2NPs, various tests are employed. These methods are utilized to evaluate the scavenging ability of antioxidants in a range of foods, including juices, vegetables, extracts and biosynthesized nanomaterials. They are appreciated for being straightforward, cost-effective and highly sensitive [54, 57].

Figure 6 shows that the antioxidant power of biosynthesized CeO_2NPs increased significantly at five different concentrations (10, 50, 100, 150 and 200 µg/mL). The spectrophotometric DPPH scavenging assay quantifies the ability of these nanoparticles to neutralize DPPH free radicals. At a concentration of 200 µg/mL, the DPPH activity of CeO_2NPs was measured at $74.68 \pm 1.39\%$. The IC_{50} value for DPPH was found to be 107.16 µg/mL, compared to a positive control value of 79.88 µg/mL. The ABTS assay showed an antioxidant potential of $70.85 \pm 1.28\%$ at the same concentration. The IC_{50} value for ABTS was 122.93 µg/mL and the value for the positive control was 100.66 µg/mL. The H_2O_2 and SOD tests showed that 200 µg/mL of CeO_2NPs effectively got rid of radicals, with activities of $68.72 \pm 1.29\%$ and $63.47 \pm 1.14\%$, respectively. The IC_{50} values for H_2O_2 were 130.05 µg/mL, while the positive control was 109.68 µg/mL and for SOD, the IC_{50} values were 144.12 µg/mL, with a positive control of 116.82 µg/mL. Also, CeO_2NPs had RPA activities of $72.94 \pm 1.29\%$ and FRAP activities of $65.58 \pm 1.24\%$ at 200 µg/mL. The IC_{50} values for RPA were 111.34 µg/mL and the positive control was 91.04 µg/mL. The 131.88 µg/mL for FRAP and the positive control was 114.73 µg/mL. Overall, the DPPH test showed that the 200 µg/mL concentration of CeO_2NPs had the highest antioxidant potential ($74.68 \pm 1.39\%$). Furthermore, we found a direct correlation between an increase in CeO_2NPs concentration and an enhancement in their reducing potential across all antioxidant activities.

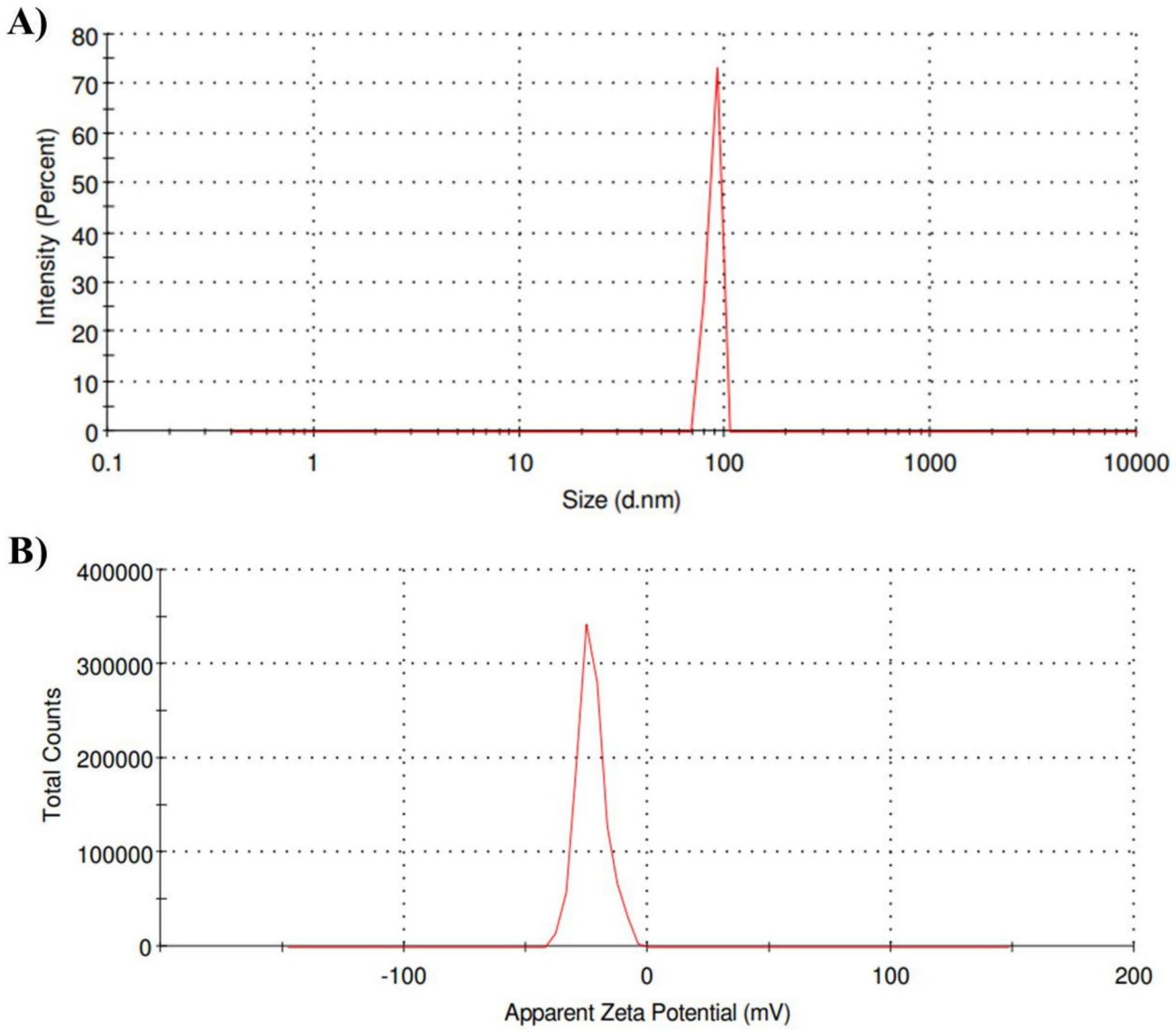

Fig. 5 **A** DLS analysis and (**B**) Zeta potential analysis of synthesized CeO_2NPs

A study found that CeO_2NPs green made from *Abelmoschus esculentus* extract had the highest antioxidant activity (88.15%) when diluted to 100 µg/mL [58]. According to Pandiyan et al. [25], SrO/CeO_2NPs made from *P. murex* leaf extract had the highest antioxidant activity of 89%. Additionally, research showed that green CeO_2NPs synthesized from *Oroxylum indicum* seed extract demonstrated a maximum scavenging activity of 63.4 ± 3.17% at 100 µg/mL [30]. Biogenically, CeO_2NPs made from *Origanum majorana* leaf extract increased the levels of catalase and superoxide dismutase, showing better antioxidant activity [28]. Also, CeO_2NPs made from *Ceratonia siliqua* extracts showed antioxidant properties that changed with dose, with higher concentrations showing the most antioxidant potential. Remarkably, these CeO_2NPs showed superior antioxidant activity in comparison to this study [29].

Antibacterial Activity

The antibacterial efficacy of biosynthesized CeO_2NPs was evaluated against five pathogenic bacteria, including *S. aureus, B. subtilis, E. coli, K. pneumonia* and *S. typhi*. The results showed that synthesized CeO_2NPs were very

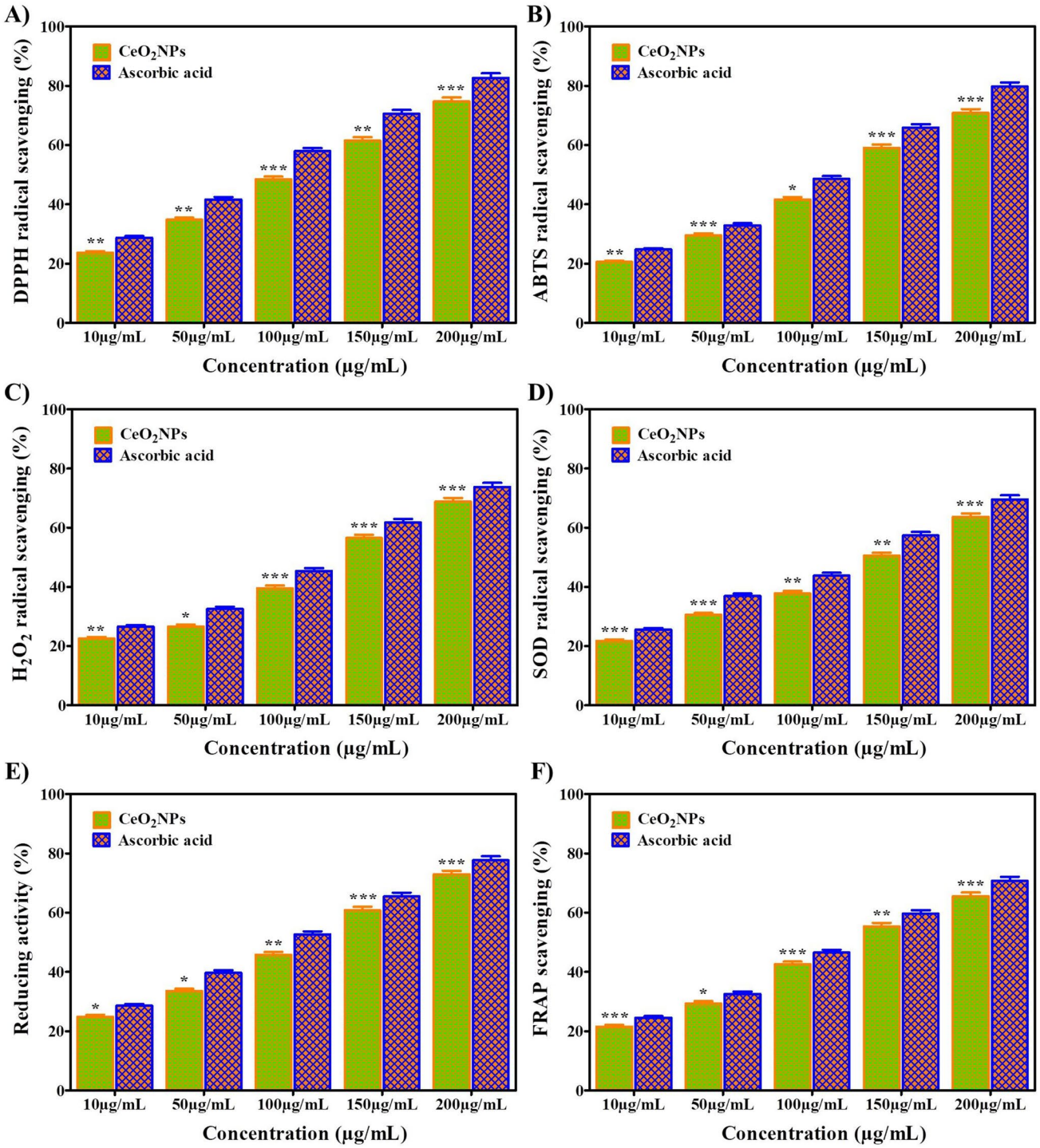

Fig. 6 Antioxidant activity of (**A**) DPPH, **B** ABTS, **C** H_2O_2, **D** SOD, **E** RPA and **F** FRAP for synthesized CeO_2NPs at various concentrations. Values are expressed as mean ± SD (*p < 0.05; **p < 0.001; ***p < 0.0001). An asterisk signifies significant differences when compared to the control group

effective at killing all strains of bacteria that were tested at a concentration of 200 µg/mL (Table 1). It's worth mentioning that CeO_2NPs had the highest ZOI against *S. aureus* (23.97 ± 1.29 mm), *B. subtilis* (21.38 ± 1.16 mm), *E. coli* (25.04 ± 1.45 mm), *K. pneumoniae* (22.90 ± 1.21 mm) and *S. typhi* (19.78 ± 1.06 mm) when compared to the positive control. The antibacterial effects were statistically superior to those of the positive control. *E. coli* (25.04 ± 1.45 mm)

Table 1 The antibacterial activity of synthesized CeO_2NPs at different concentrations against gram-positive and gram-negative bacteria

Name of the pathogens	Zone of Inhibition (mm) Concentration (µg/mL)				
	PC	10	50	100	200
S. aureus	22.73 ± 1.24	15.29 ± 0.35*	17.82 ± 0.51**	20.61 ± 0.86***	23.97 ± 1.29***
B. subtilis	20.58 ± 1.17	13.74 ± 0.28**	16.13 ± 0.47*	18.92 ± 0.74**	21.38 ± 1.16***
E. coli	24.94 ± 1.34	16.89 ± 0.42**	18.64 ± 0.85***	21.49 ± 1.32**	25.04 ± 1.45***
K. pneumonia	21.49 ± 1.07	14.28 ± 0.31***	17.93 ± 0.56**	19.38 ± 0.83***	22.90 ± 1.21***
S. typhi	19.38 ± 0.95	12.41 ± 0.25*	14.59 ± 0.41**	16.71 ± 0.52**	19.78 ± 1.06***

Values are expressed as mean ± SD (*p < 0.05; **p < 0.001; ***p < 0.0001)

An asterisk signifies significant differences when compared to the control group

have the highest ZOI in comparison to the other strains. The pronounced antibacterial activity against the bacteria suggests that the cell wall plays a crucial role in the susceptibility of these bacterial species to CeO_2NPs. Bacteria can bind and take in negatively charged CeO_2NPs better because they have a lot of cell surface proteins and teichoic acids [32]. Furthermore, the particle size, high surface-to-volume ratio and ROS generation of CeO_2NPs contribute to their antibacterial properties. Multiple studies have elucidated the antibacterial mechanisms of nanoparticles, which disrupt the bacterial cell membrane, cytoplasm and nucleic acids, ultimately compromising cellular integrity and leading to cell death [59, 60]. A study reported that the biosynthesis of CeO_2NPs at 100 µg/mL exhibited the highest ZOI of *E. coli* (22 ± 0.3), as observed [54]. Another study reported that the synthesis of CeO_2NPs using *Aloe vera* leaf extract, at 75 µg/mL, exhibited the highest ZOI of *S. aureus* (22.33 ± 1.67), as observed [61].

Anti-Inflammatory Activity

The body uses inflammation as a systematic response to defend itself against harmful agents such as bacteria, irritants, adverse stimuli and damaged cells [62]. The anti-inflammatory qualities of several metallic nanoparticles and secondary metabolites have been shown in numerous in vitro and in vivo investigations. Flavonoid compounds, such as vitexin, isovitexin, orientin and isoorientin, may be used in the biosynthesis of NPs [47, 63]. These compounds are known for their strong anti-inflammatory properties. These flavonoids work against cyclooxygenase (COX-1 and COX-2) and other related enzymes. This lowers the levels of inflammation-causing prostanoids and leukotrienes. Current and emerging therapies aim to address inflammatory disorders by significantly alleviating symptoms [64]. Notably, metallic NPs possess a unique ability to penetrate microbial cell membranes, which can enhance the delivery of specific drugs during microbial infections. Recent scientific advancements focus on synthesizing NPs designed to manage inflammatory conditions through the incorporation of anti-inflammatory

Table 2 CeO_2NPs demonstrated anti-inflammatory activity at varying concentrations for COX-1 and COX-2

Name of the drug	Conc. (µg/mL)	Inhibition (%)			
		COX-1	IC_{50}	COX-2	IC_{50}
Ibuprofen	10	28.83 ± 0.46		25.18 ± 0.52	
	50	39.61 ± 0.62		36.62 ± 0.71	
	100	55.92 ± 0.85	78.60 µg/mL	51.49 ± 0.93	92.23 µg/mL
	150	74.29 ± 1.13		69.21 ± 1.12	
	200	89.36 ± 1.38		82.47 ± 1.26	
CeO_2NPs	10	22.58 ± 0.49**		19.35 ± 0.41***	
	50	32.75 ± 0.65***		28.59 ± 0.54*	
	100	48.32 ± 0.84*	101.34 µg/mL	41.73 ± 0.82**	125.07 µg/mL
	150	66.47 ± 1.06**		56.82 ± 0.96***	
	200	80.91 ± 1.22***		71.58 ± 1.16***	

Ibuprofen was used as a positive control

Values are expressed as mean ± SD (*p < 0.05; **p < 0.001; ***p < 0.0001)

An asterisk signifies significant differences when compared to the control group

agents [65]. The anti-inflammatory efficacy of CeO_2NPs was evaluated using various in vitro assays, including COX-1 and COX-2. Results from these assays revealed strong inhibitory activity across all tested CeO_2NPs at various concentrations. Table 2 showed that CeO_2NPs (200 µg/mL) had the highest inhibitory activity of COX-1 (80.91 ± 1.22%), followed by COX-2 (71.58 ± 1.16%). IC_{50} values of COX-1 exhibit 101.34 µg/mL and the positive control for 78.60 µg/mL. The COX-2 IC_{50} value is 125.07 µg/mL and the positive control is 92.23 µg/mL. Overall, the results show that CeO_2NPs (200 µg/mL) can effectively block both COX-1 and COX-2 enzymes, which are important in inflammatory processes.

Antidiabetic Activity

Diabetes mellitus is a high-risk metabolic disorder characterized by prolonged elevated blood sugar levels, along with disrupted metabolism of fats, proteins and carbohydrates. Inhibiting carbohydrate-metabolizing enzymes, especially α-amylase and α-glucosidase, strongly is an effective way to treat diabetes [66]. Chemical medicines like acarbose and voglibose stop these enzymes from working, which stops disaccharides from turning into monosaccharaides and lowers the amount of glucose that gets into the bloodstream [67]. However, these synthetic drugs are associated with various side effects. Therefore, researchers are becoming more interested in natural inhibitors that come from plants. These inhibitors may work well against these enzymes because they contain many different phenolic compounds, alkaloids, terpenes and other bioactive substances [68].

This study found that green synthesized CeO_2NPs blocked α-amylase more effectively than α-glucosidase (Fig. 7). A significant dose-dependent response was seen in the antidiabetic potential linked to the inhibitory activity of these enzymes as the concentration of CeO_2NPs rose. At a concentration of 200 µg/mL of CeO_2NPs, the enzymes α-amylase and α-glucosidase were found to show 70.46 ± 1.37% and 79.58 ± 1.37% inhibition activity, respectively (Fig. 7A, B). The calculated IC_{50} values for CeO_2NPs againstα-amylase were 109.38 µg/mL, while the positive control was 74.98 µg/mL. For α-glucosidase, the IC_{50} values for CeO_2NPs were determined to be 916.8 µg/mL, with the positive control at 69.30 µg/mL. Manasa et al. [69] have also reported similar antidiabetic effects of ZnONPs from the *Tabernaemontana heyneana* plant extract. The results show that the biofabricated CeO_2NPs are good at blocking enzymes that break down carbohydrates. This suggests that they might be useful for managing diabetes mellitus well.

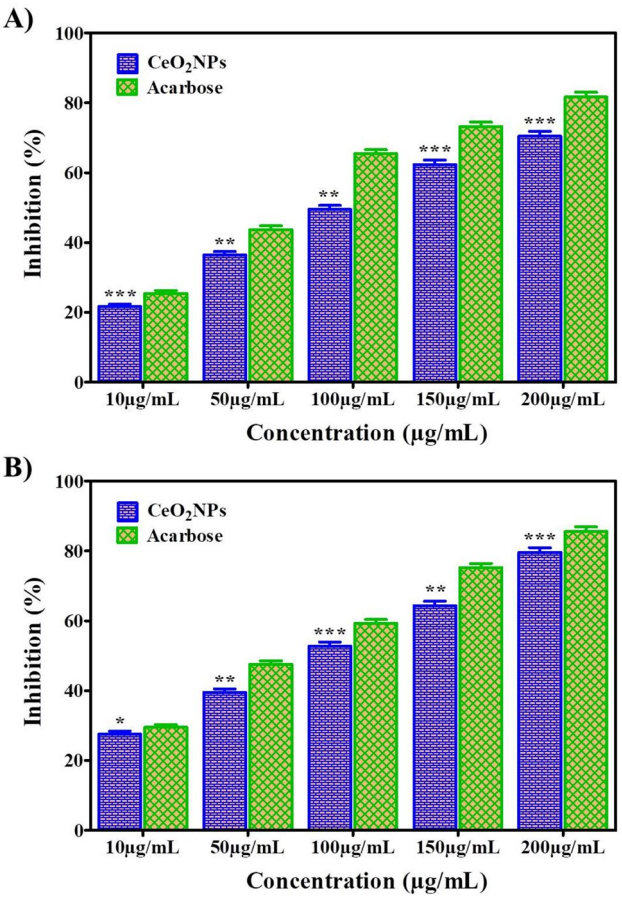

Fig. 7 The synthesized CeO_2NPs antidiabetic activity of (**A**) α-amylase activity and (**B**) α-glucosidase activity at different concentrations. Values are expressed as mean ± SD (*$p < 0.05$; **$p < 0.001$; ***$p < 0.0001$). An asterisk signifies significant differences when compared to the control group

Cholinesterase Inhibition Activity

Alzheimer's disease (AD) is a common and devastating neurodegenerative disorder that typically results in dementia and declining cognitive functions, which generally worsen with age [70]. Current therapeutic strategies for effectively treating Alzheimer's involve the use of various synthetic and natural molecules to inhibit cholinesterase enzymes responsible for the disease [71]. Nanotechnology, a vast field, holds promise for developing new treatment methods, including drug delivery systems. In this study, we evaluated the inhibition potential of biosynthesized CeO_2NPs on AChE and BChE. The CeO_2NPs were tested across a concentration range of 10 µg/mL to 200 µg/mL. The highest enzyme inhibition observed was 68.92 ± 1.39% for AChE and 73.47 ± 1.53% for BChE at 200 µg/mL (Fig. 8A, B). The calculated IC_{50} values were 131.78 µg/mL for AChE and 106.90 µg/mL for BChE. Previous studies have shown that several metallic nanoparticles can inhibit AChE and BChE.

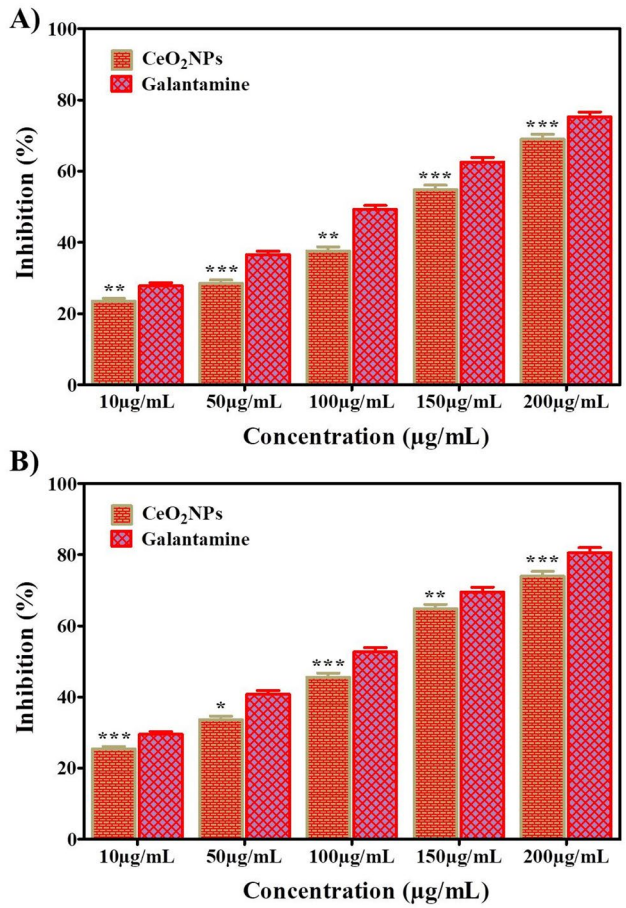

Fig. 8 The synthesized CeO_2NPs for the anticholinergic activity of (**A**) AChE activity and (**B**) BChE activity at various concentrations. Values are expressed as mean ± SD (*p < 0.05; **p < 0.001; ***p < 0.0001). An asterisk signifies significant differences when compared to the control group

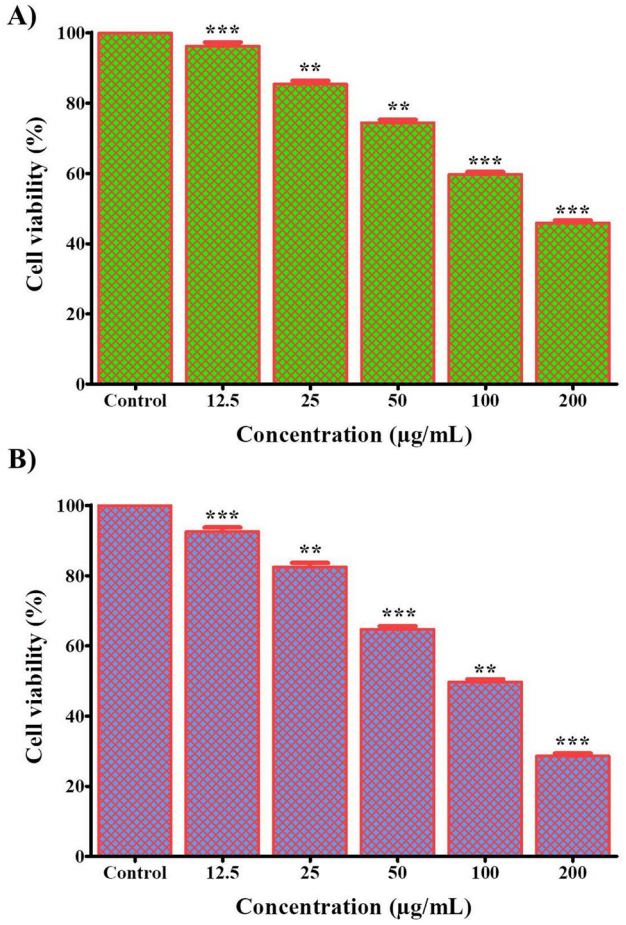

Fig. 9 Cell viability assay of synthesized CeO_2NPs for HepG2 cell lines (**A**) 24 h and (**B**) 48 h for various concentrations. Values are expressed as mean ± SD (*p < 0.05; **p < 0.001; ***p < 0.0001). An asterisk signifies significant differences when compared to the control group

Notably, biosynthesized magnesium hydroxide nanoparticles demonstrated significant inhibition of cholinesterase activity by 70.93% (AChE) and 87.94% (BChE) at 200 µg/mL [72]. Also, silver nanoparticles made from *Aquilegia pubiflora* plant extract stopped AChE and BChE from working by 71% and 67%, respectively [73].

Cytotoxicity Assay

The hallmark of cancer is the uncontrolled proliferation of cells. Liver cancer is the sixth most frequent type of cancer worldwide, and it causes about 700,000 deaths annually [74]. Liver cancer can be treated with surgery, liver transplantation, targeted therapies, interventional therapies, radiofrequency ablation, chemotherapy and microwave ablation. Nanotechnology and chemicals derived from plants have recently drawn more attention as potential treatments for hepatocellular cancer [75]. Reports indicate that biosynthesized NPs demonstrate significant anti-cancer activity against the HepG2 cell line, indicating their potential for developing liver cancer therapeutics [47, 76].

This study used biosynthesized CeO_2ONPs to target the HepG2 cancer cell line (Fig. 9). After 24 h of incubation, a dose-dependent decrease in cell viability was observed, with a reduction of 45.92 ± 0.69% at 200 µg/mL (Fig. 9A). The maximum concentration of CeO_2NPs (200 µg/mL) resulted in a 28.59 ± 0.39% decrease in cell viability compared to the control after 48 h (Fig. 9B). The survival features of cancer cells are distinct from those of normal cells. Biosynthetic iron oxide nanoparticles prepared from *Cocos nucifera* extract showed anti-cancer activity against HepG2 cells, reducing cell viability by up to 68.87% [77]. Ashraf et al. [78] also found that green ZnONPs made from *Boerhavia diffusa Linn* extract effectively stopped HepG2 cell growth, resulting in 33 ± 1.61% cell viability, showing that they could be a promising therapeutic approach.

Conclusion

The current study highlights the biosynthesis of CeO_2NPs using environmentally friendly green techniques with an aqueous extract from *A. sessilis* plants. This approach is characterized as a simple, safe, eco-friendly and one-step process, thereby promoting the adoption of photosynthesis for the preparation of other metal oxide nanoparticles. The biogenic CeO_2NPs display a distinct UV–Vis spectrum absorption range at 326 nm. FTIR spectrum analysis revealed various functional groups, while XRD analysis confirmed the crystalline structure of the CeO_2NPs. The FESEM and HR-TEM methods confirmed the presence of CeO_2NPs, which had spherical and oval shapes and an average particle size of 29 nm. Zeta potential studies confirm that the synthesized CeO_2NPs have a negative charge of -28 mV. These nanoparticles exhibited strong antioxidant properties and demonstrated effective antibacterial activity. Additionally, the CeO_2NPs demonstrated strong anti-inflammatory potential by inhibiting the enzymes COX-1 and COX-2, which cause inflammation. Furthermore, biological tests showed that the biosynthesized CeO_2NPs have strong inhibitory effects on enzymes that cause antidiabetic and anti-cholinergic activities. The cytotoxicity tests showed that these CeO_2NPs are harmful to HepG2 cancer cells, as shown by a significant drop in cell viability. In summary, the green synthesis of CeO_2NPs presents a non-toxic, cost-effective and safe approach, positioning them as a highly promising option for various biological applications.

Acknowledgements This work was financially supported by a Post-Doctoral Fellow (PDF) from SSN College of Engineering, Chennai-603 110, Tamil Nadu, India (SSN/CE/PDF/2024).

Author Contributions M.R: Methodology, Investigation, Software analysis, Writing – original draft. S.I.D.P: Supervision, Investigation, Writing – review & editing, Conceptualization. P.G, K.M and C.R: Methodology, Data curation, Software analysis. M.M.A and F.M: Data curation, Formal analysis, Software analysis.

Funding SSN College of Engineering,SSN/CE/PDF/2024,Manickam Rajkumar

Data Availability Data are available upon request from the authors.

Declarations

Conflict of interest The authors declare that they have no known competing financial interests or personal relationships that could have appeared to influence the work reported in this paper.

Informed Consent Not applicable.

Human and Animal Rights Statement Not applicable.

References

1. N.B. Singh, B. Kumar, U.L. Usman, M.A.B.H. Susan, Nano revolution: exploring the frontiers of nanomaterials in science, technology, and society. Nano-Struct. Nano-Obj. **39**, 101299 (2024)
2. T.T. Truong, S. Mondal, V.H.M. Doan, S. Tak, J. Choi, H. Oh, T.D. Nguyen, M. Misra, B. Lee, J. Oh, Precision-engineered metal and metal-oxide nanoparticles for biomedical imaging and healthcare applications. Adv. Colloid Interface Sci. (2024). https://doi.org/10.1016/j.cis.2024.103263
3. K.R. Singh, V. Nayak, J. Singh, A.K. Singh, R.P. Singh, Potentialities of bioinspired metal and metal oxide nanoparticles in biomedical sciences. RSC Adv. **11**, 24722–24746 (2021)
4. L. Saghatforoush, T. Mahmoudi, Z. Khorablou, H. Nasiri, A. Bakhtiari, S.A.A. Sajadi, Electro-oxidation sensing of sumatriptan in aqueous solutions and human blood serum by Zn (II)-MOF modified electrochemical delaminated pencil graphite electrode. Sci. Rep. **13**(1), 16803 (2023)
5. A. Goswami, S. Garg, E. Bhatt, V. Chaudhary, S. Dang, Nanotechnology-based biosensors for biomedical applications. J. Electrochem. Soc. **171**(9), 097508 (2024)
6. H. Nasiri, K. Abbasian, M. Salahandish, S.N. Elyasi, Sensitive surface plasmon resonance biosensor by optimized carboxylate functionalized carbon nanotubes/chitosan for amlodipine detecting. Talanta **276**, 126249 (2024)
7. H. Nasiri, H. Baghban, R. Teimuri-Mofrad, A. Mokhtarzadeh, Graphitic carbon nitride/magnetic chitosan composite for rapid electrochemical detection of lactose. Int. Dairy J. **136**, 105489 (2023)
8. J.A. Kumar, T. Krithiga, S. Manigandan, S. Sathish, A.A. Renita, P. Prakash, B.N. Prasad, T.P. Kumar, M. Rajasimman, A. Hosseini-Bandegharaei, D. Prabu, A focus to green synthesis of metal/metal based oxide nanoparticles: various mechanisms and applications towards ecological approach. J. Cleaner Prod. **324**, 129198 (2021)
9. D. Kirubakaran, K. Selvam, M. Dhaneeshram, M.S. Shivakumar, M. Rajkumar, A. Shanmugarathinam, Biogenic synthesis of copper nanoparticle using Impatiens chinensis L: insights into antimicrobial, antioxidant and anticancer activity. J. Mol. Struct. **1317**, 138991 (2024)
10. V. Harish, D. Tewari, M. Gaur, A.B. Yadav, S. Swaroop, M. Bechelany, A. Barhoum, Review on nanoparticles and nanostructured materials: bioimaging, biosensing, drug delivery, tissue engineering, antimicrobial, and agro-food applications. Nanomaterials **12**(3), 457 (2022)
11. M. Rajkumar, D. Kirubakaran, K. Selvam, N. Prathap, R. Thangaraj, K. Vimala, S. Kannan, Green synthesis of gelatin-loaded magnesium hydroxide nanocomposite biomaterial using *Coleus amboinicus* leaf extract for enhanced antibacterial, antioxidant, anticholinergic, and wound healing activities. J. Mater. Res. **39**(4), 548–564 (2024)
12. M.S. Samuel, M. Ravikumar, J.A. John, E. Selvarajan, H. Patel, P.S. Chander, J. Soundarya, S. Vuppala, R. Balaji, N. Chandrasekar, A review on green synthesis of nanoparticles and their diverse biomedical and environmental applications. Catalysts **12**(5), 459 (2022)
13. M. Nasrollahzadeh, S. Mahmoudi-Gom Yek, N. Motahharifar, M. Ghafori Gorab, Recent developments in the plant-mediated green synthesis of Ag-based nanoparticles for environmental and catalytic applications. Chem. Rec. **19**(12), 2436–2479 (2019)
14. A. Gauba, S.K. Hari, V. Ramamoorthy, S. Vellasamy, G. Govindan, M.V. Arasu, The versatility of green synthesized zinc oxide nanoparticles in sustainable agriculture: a review on metal-microbe interaction that rewards agriculture. Physiol. Mol. Plant Pathol. **125**, 102023 (2023)

15. R. Atchudan, S. Perumal, S.C. Kishore, A.K. Sundramoorthy, D. Manoj, S. Sambasivam, R.S. Kumar, M. Alagan, S. Ramalingam, S.W. Lee, Y.R. Lee, Sustainable synthesis of multi-functional carbon dots as optical nanoprobe for selective sensing of heavy metal ions. J. Taiwan Inst. Chem. Eng. **165**, 105770 (2024)
16. E. Ibrahim, L. Xu, R. Nasser, A.S.M. Adel, R. Hafeez, S.O. Ogunyemi, Y. Abdallah, Z. Zhang, L. Shou, D. Wang, B. Li, Utilizing zinc oxide nanoparticles as an environmentally safe biosystem to mitigate mycotoxicity and suppress Fusarium graminearum colonization in wheat. Sustain. Mater. Technol. **41**, e01028 (2024)
17. K. Senthilkumar, M. Rajkumar, K. Vimala, R. Thangaraj, S. Kannan, Biosynthesis of gelatin-coated zinc oxide nanocomposites from *Coccinia indica* extract and its antibacterial, antioxidant, anticancer wound healing properties. BioNanoScience **14**(3), 2993–3010 (2024)
18. A.F. Burlec, A. Corciova, M. Boev, D. Batir-Marin, C. Mircea, O. Cioanca, G. Danila, M. Danila, A.F. Bucur, M. Hancianu, Current overview of metal nanoparticles' synthesis, characterization, and biomedical applications, with a focus on silver and gold nanoparticles. Pharmaceutics **16**(10), 1410 (2023)
19. D. Kirubakaran, K. Selvam, P. Prakash, M.S. Shivakumar, M. Rajkumar, In-vitro antioxidant, antidiabetic, anticholinergic activity of iron/copper nanoparticles synthesized using *Strobilanthes cordifolia* leaf extract. OpenNano **14**, 100188 (2023)
20. H. Nasiri, K. Abbasian, High-sensitive surface plasmon resonance sensor for melamine detection in dairy products based on graphene oxide/chitosan nanocomposite. Food Control **166**, 110761 (2024)
21. H. Nasiri, K. Abbasian, H. Baghban, Sensing of lactose by graphitic carbon nitride/magnetic chitosan composites with surface plasmon resonance method. Food Biosci. **61**, 104718 (2024)
22. H. Nasiri, H. Baghban, R. Teimuri-Mofrad, A. Mokhtarzadeh, Chitosan/polyaniline/graphene oxide-ferrocene thin film and highly-sensitive surface plasmon sensor for glucose detection. Opt. Quantum Electron. **55**(11), 948 (2023)
23. M.H. Emam, R.S. Elezaby, S.A. Swidan, S.A. Loutfy, R.M. Hathout, Cerium oxide nanoparticles/polyacrylonitrile nanofibers as impervious barrier against viral infections. Pharmaceutics **15**(5), 1494 (2023)
24. T.U. Haq, R. Ullah, M.N. Khan, S. Wahab, B. Ali, A. Kaplan, M.A. Javed, Phyto-drug (Silymarin)-encapsulated cerium oxide nanoparticles (S-CeONP s) for in-vitro release, ameliorating antimicrobial, anticancer, anti-inflammatory and antioxidant potential. BioNanoScience (2024). https://doi.org/10.1007/s12668-023-01295-8
25. N. Pandiyan, B. Murugesan, J. Sonamuthu, S. Samayanan, S. Mahalingam, [BMIM] PF6 ionic liquid mediated green synthesis of ceramic SrO/CeO2 nanostructure using *Pedalium murex* leaf extract and their antioxidant and antibacterial activities. Ceram. Int. **45**(9), 12138–12148 (2019)
26. R. Javed, R. Ghonaim, A. Shathili, S.A. Khalifa, H.R. El-Seedi, Phytonanotechnology: A greener approach for biomedical applications, in Biogenic Nanoparticles for Cancer Theranostics 43–86 (2021)
27. A. Miri, M. Darroudi, M. Sarani, Biosynthesis of cerium oxide nanoparticles and its cytotoxicity survey against colon cancer cell line. Appl. Organomet. Chem. **34**(1), e5308 (2020)
28. S. Aseyd Nezhad, A. Es-haghi, M.H. Tabrizi, Green synthesis of cerium oxide nanoparticle using *Origanum majorana* L. leaf extract, its characterization and biological activities. Appl. Organomet. Chem. **34**(2), e5314 (2020)
29. F. Javadi, M.E.T. Yazdi, M. Baghani, A. Es-haghi, Biosynthesis, characterization of cerium oxide nanoparticles using *Ceratonia siliqua* and evaluation of antioxidant and cytotoxicity activities. Mater. Res. Express **6**(6), 065408 (2019)
30. J. Mim, M.S. Sultana, P.K. Dhar, M.K. Hasan, S.K. Dutta, Green mediated synthesis of cerium oxide nanoparticles by using *Oroxylum indicum* for evaluation of catalytic and biomedical activity. RSC Adv. **14**(35), 25409–25424 (2024)
31. N.C. Joshi, T. Negi, P. Gururani, Papaya (*Carica papaya*) leaves extract based synthesis, characterizations and antimicrobial activities of CeO2 nanoparticles (CeO2 NPs). Inorg. Nano-Met. Chem. (2023). https://doi.org/10.1080/24701556.2023.2166068
32. S. Pansambal, R. Oza, S. Borgave, A. Chauhan, P. Bardapurkar, S. Vyas, S. Ghotekar, Bioengineered cerium oxide (CeO2) nanoparticles and their diverse applications: a review. Appl. Nanosci. **13**(9), 6067–6092 (2023)
33. A.K. Mandal, D.K. Gopi, S.K. Narayana, K.C.H.S. Ramachandran, Fingerprints of two medicinal species of alternanthera–a ficoidea and a sessilis to facilitate differentiation in dried form. Indian J. Nat. Prod. Resour. **13**(4), 525–536 (2023)
34. M.I. Yatoo, A. Gopalakrishnan, A. Saxena, O.R. Parray, N.A. Tufani, S. Chakraborty, R. Tiwari, K. Dhama, H.M. Iqbal, Anti-inflammatory drugs and herbs with special emphasis on herbal medicines for countering inflammatory diseases and disorders—a review. Recent Pat. Inflamm. Allergy Drug Discov. **12**(1), 39–58 (2018)
35. O. Ragavan, S.C. Chan, Y.E. Goh, V. Lim, Y.K. Yong, *Alternanthera sessilis*: a review of literature on the phytoconstituents, traditional usage and pharmacological activities of green and red cultivar. Pharmacogn. Res. (2023). https://doi.org/10.5530/pres.15.4.067
36. C.S. Hwong, K.H. Leong, A.A. Aziz, S.M. Junit, S.M. Noor, K.W. Kong, *Alternanthera sessilis*: uncovering the nutritional and medicinal values of an edible weed. J. Ethnopharmacol. **298**, 115608 (2022)
37. A. Abdelkhalek, A.A. Al-Askar, Green synthesized ZnO nanoparticles mediated by Mentha spicata extract induce plant systemic resistance against tobacco mosaic virus. Appl. Sci. **10**(15), 5054 (2020)
38. R. Wołosiak, B. Drużyńska, D. Derewiaka, M. Piecyk, E. Majewska, M. Ciecierska, E. Worobiej, P. Pakosz, Verification of the conditions for determination of antioxidant activity by ABTS and DPPH assays—a practical approach. Molecules **27**(1), 50 (2021)
39. C.D. Fernando, P. Soysa, Optimized enzymatic colorimetric assay for determination of hydrogen peroxide (H2O2) scavenging activity of plant extracts. MethodsX **2**, 283–291 (2015)
40. O. Vajragupta, P. Boonchoong, L.J. Berliner, Manganese complexes of *curcumin analogues*: evaluation of hydroxyl radical scavenging ability, superoxide dismutase activity and stability towards hydrolysis. Free Radic. Res. **38**(3), 303–314 (2004)
41. F. Odabasoglu, A. Aslan, A. Cakir, H. Suleyman, Y. Karagoz, Y. Bayir, M. Halici, Antioxidant activity, reducing power and total phenolic content of some lichen species. Fitoterapia **76**(2), 216–219 (2005)
42. C. Guo, J. Yang, J. Wei, Y. Li, J. Xu, Y. Jiang, Antioxidant activities of peel, pulp and seed fractions of common fruits as determined by FRAP assay. Nutr. Res. **23**(12), 1719–1726 (2003)
43. J.J. Biemer, Antimicrobial susceptibility testing by the Kirby-Bauer disc diffusion method. Ann. Clin. Lab. Sci. **3**(2), 135–140 (1973)
44. A. Tanaka, S. Hase, T. Miyazawa, R. Ohno, K. Takeuchi, Role of cyclooxygenase (COX)-1 and COX-2 inhibition in nonsteroidal anti-inflammatory drug-induced intestinal damage in rats: relation to various pathogenic events. J. Pharmacol Exp. Ther. **303**(3), 1248–1254 (2002)
45. C. Gu, H. Zhang, C.Y. Putri, K. Ng, Evaluation of α-amylase and α-glucosidase inhibitory activity of flavonoids. Int. J. Food Nutr. Sci. **2**, 1–6 (2015)

46. G. Sinko, M. Calic, A. Bosak, Z. Kovarik, Limitation of the Ellman method: Cholinesterase activity measurement in the presence of oximes. Anal. Biochem. **370**(2), 223–227 (2007)
47. H. Jan, M. Shah, A. Andleeb, S. Faisal, A. Khattak, M. Rizwan, S. Drouet, C. Hano, B.H. Abbasi, Plant-based synthesis of zinc oxide nanoparticles (ZnO-NPs) using aqueous leaf extract of *Aquilegia pubiflora*: their antiproliferative activity against HepG2 cells inducing reactive oxygen species and other in vitro properties. Oxid. Med. Cell. Longev. (2021). https://doi.org/10.1155/2021/4786227
48. S. Surendhiran, K.S. Balu, A. Karthik, V. Rajendran, Biogenic synthesis of CeO2 nanoparticles via moringa oleifera seed extract: photocatalytic and biological activity for textile dye degradation. J. Indian Chem. Soc. **101**(10), 101302 (2024)
49. J. Sukumaran, R. Venkatesan, M. Priya, S.C. Kim, Eco-friendly synthesis of CeO2 nanoparticles using Morinda citrifolia L leaf extracts: evaluation of structural, antibacterial, and anti-inflammatory activity. Inorg. Chem. Commun. (2024). https://doi.org/10.1016/j.inoche.2024.113411
50. S. Nag, O. Mitra, P. Sankarganesh, A. Bhattacharjee, S. Mohanto, B.J. Gowda, S. Kar, S. Ramaiah, A. Anbarasu, M.G. Ahmed, Exploring the emerging trends in the synthesis and theranostic paradigms of cerium oxide nanoparticles (CeONPs): a comprehensive review. Mater. Today Chem. **35**, 101894 (2024)
51. S. Safat, F. Buazar, S. Albukhaty, S. Matroodi, Enhanced sunlight photocatalytic activity and biosafety of marine-driven synthesized cerium oxide nanoparticles. Sci. Rep. **11**(1), 14734 (2021)
52. Q. Maqbool, M. Nazar, S. Naz, T. Hussain, N. Jabeen, R. Kausar, S. Anwaar, F. Abbas, T. Jan, Antimicrobial potential of green synthesized CeO2 nanoparticles from *Olea europaea* leaf extract. Int. J. Nanomed. **11**, 5015–5025 (2016)
53. S. Chaturvedi, D. Maheshwari, A. Chawathe, N. Sharma, Current analytical approaches for characterizing nanoparticle sizes in pharmaceutical research. J. Nanoparticle Res. **26**(1), 19 (2024)
54. A. Muthuvel, M. Jothibas, C. Manoharan, S.J. Jayakumar, Synthesis of CeO2-NPs by chemical and biological methods and their photocatalytic, antibacterial and in vitro antioxidant activity. Res. Chem. Intermed. **46**, 2705–2729 (2020)
55. I.Z. Sadiq, Free radicals and oxidative stress: Signaling mechanisms, redox basis for human diseases, and cell cycle regulation. Curr. Mol. Med. **23**(1), 13–35 (2023)
56. J. Xie, R. Dong, T. Zhang, F. Guo, H. Li, X. Chen, Y. Wu, X. Zhang, Y. Yong, Z. Gu, Natural dietary ROS scavenger-based nanomaterials for ROS-related chronic disease prevention and treatment. Chem. Eng. J. **490**, 151756 (2024)
57. N.S. Al-Radadi, Laboratory scale medicinal plants mediated green synthesis of biocompatible nanomaterials and their versatile biomedical applications. Saudi J. Biol. Sci. **29**(5), 3848–3870 (2022)
58. H.E. Ahmed, Y. Iqbal, M.H. Aziz, M. Atif, Z. Batool, A. Hanif, N. Yaqub, W.A. Farooq, S. Ahmad, A. Fatehmulla, H. Ahmad, Green synthesis of CeO2 nanoparticles from the *Abelmoschus esculentus* extract: evaluation of antioxidant, anticancer, antibacterial, and wound-healing activities. Molecules **26**(15), 4659 (2021)
59. S. Yefimova, V. Klochkov, N. Kavok, A. Tkachenko, A. Onishchenko, T. Chumachenko, N. Dizge, S. Ozdemir, S. Gonca, K. Ocakoglu, Antimicrobial activity and cytotoxicity study of cerium oxide nanoparticles with two different sizes. J. Biomed. Mater. Res. B Appl. Biomater. **111**(4), 872–880 (2023)
60. M. Godoy-Gallardo, U. Eckhard, L.M. Delgado, Y.J. de Roo Puente, M. Hoyos-Nogués, F.J. Gil, R.A. Perez, Antibacterial approaches in tissue engineering using metal ions and nanoparticles: from mechanisms to applications. Bioact. Mater. **6**(12), 4470–4490 (2021)
61. A.N. Shetty, K.K. Desai, S.C. Patil, Green combustion synthesis of CeO2 nanostructure using *Aloe vera* (L.) Burm f. Leaf gel and their structural, optical and antimicrobial applications. Bionanoscience. **12**(3), 757–765 (2022)
62. K.B. Megha, X. Joseph, V. Akhil, P.V. Mohanan, Cascade of immune mechanism and consequences of inflammatory disorders. Phytomedicine **91**, 153712 (2021)
63. H. Agarwal, A. Nakara, V.K. Shanmugam, Anti-inflammatory mechanism of various metal and metal oxide nanoparticles synthesized using plant extracts: a review. Biomed. Pharmacother. **109**, 2561–2572 (2019)
64. K. Bashir Dar, A. Hussain Bhat, S. Amin, A. Masood, M. Afzal Zargar, S. Ahmad Ganie, Inflammation: a multidimensional insight on natural anti-inflammatory therapeutic compounds. Curr. Med. Chem. **23**(33), 3775–3800 (2016)
65. D. Placha, J. Jampilek, Chronic inflammatory diseases, anti-inflammatory agents and their delivery nanosystems. Pharmaceutics **13**(1), 64 (2021)
66. S. Alam, M.K. Hasan, S. Neaz, N. Hussain, M.F. Hossain, T. Rahman, Diabetes Mellitus: insights from epidemiology, biochemistry, risk factors, diagnosis, complications and comprehensive management. Diabetology **2**(2), 36–50 (2021)
67. S. Kumari, R. Saini, A. Bhatnagar, A. Mishra, Exploring plant-based alpha-glucosidase inhibitors: promising contenders for combatting type-2 diabetes. Arch. Physiol. Biochem. (2023). https://doi.org/10.1080/13813455.2023.2262167
68. C.G. Awuchi, The biochemistry, toxicology, and uses of the ecologically active phytochemicals: alkaloids, terpenes, polyphenols, and glycosides. Merit. Res. J. **5**(1), 6–21 (2020)
69. D.J. Manasa, K.R. Chandrashekar, M.P. Kumar, D. Suresh, D.M. Kumar, C.R. Ravikumar, T. Bhattacharya, H.A. Murthy, Proficient synthesis of zinc oxide nanoparticles from *Tabernaemontana heyneana* Wall via green combustion method: antioxidant, anti-inflammatory, antidiabetic, anticancer and photocatalytic activities. Results Chem. **3**, 100178 (2021)
70. M. Rajkumar, K. Vimala, D.D. Tamiliniyan, R. Thangaraj, R. Jaganathan, P. Kumaradhas, S. Kannan, Gelatin/polyvinyl alcohol loaded magnesium hydroxide nanocomposite attenuates neurotoxicity and oxidative stress in Alzheimer's disease induced rats. Int. J. Biol. Macromol. **222**, 2122–2143 (2022)
71. K. Gajendra, G.K. Pratap, D.V. Poornima, M. Shantaram, G. Ranjita, Natural acetylcholinesterase inhibitors: a multi-targeted therapeutic potential in Alzheimer's disease. Eur. J. Med. Chem. Rep. **11**, 100154 (2024)
72. M. Rajkumar, S.I. Presley, F. Menaa, S.E.I. Elbehairi, M.Y. Alfaifi, A.A. Shati, A.E. Albalawi, N.A. Althobaiti, D. Kirubakaran, P. Govindaraj, K. Meenambigai, Biosynthesis and biological activities of magnesium hydroxide nanoparticles using *Tinospora cordifolia* leaf extract. Bioprocess Biosyst. Eng. **47**(12), 2111–2129 (2024)
73. H. Jan, G. Zaman, H. Usman, R. Ansir, S. Drouet, N. Gigliolo-Guivarc'h, C. Hano, B.H. Abbasi, Biogenically proficient synthesis and characterization of silver nanoparticles (Ag-NPs) employing aqueous extract of *Aquilegia pubiflora* along with their in vitro antimicrobial, anti-cancer and other biological applications. J. Mater. Res. Technol. **15**, 950–968 (2021)
74. J. Huang, V. Lok, C.H. Ngai, C. Chu, H.K. Patel, V. Thoguluva Chandraseka, L. Zhang, P. Chen, S. Wang, X.Q. Lao, L.A. Tse, Disease burden, risk factors, and recent trends of liver cancer: a global country-level analysis. Liver Cancer **10**(4), 330–345 (2021)
75. D.S. Khafaga, A.M. El-Khawaga, R.A. Elfattah Mohammed, H.K. Abdelhakim, Green synthesis of nano-based drug delivery systems developed for hepatocellular carcinoma treatment: a review. Mol. Biol. Rep. **50**(12), 10351–10364 (2023)
76. N.M. Alyami, H.M. Alyami, R. Almeer, Using green biosynthesized kaempferol-coated silver nanoparticles to inhibit cancer

cells growth: An in vitro study using hepatocellular carcinoma (HepG2). Cancer Nanotechnol. **13**(1), 26 (2022)
77. A. Rajendran, M. Alsawalha, T. Alomayri, Biogenic synthesis of husked rice-shaped iron oxide nanoparticles using coconut pulp (*Cocos nucifera* L.) extract for photocatalytic degradation of Rhodamine B dye and their in vitro antibacterial and anticancer activity. J. Saudi. Chem. Soc. **25**(9), 101307 (2021)
78. H. Ashraf, B. Meer, J. Iqbal, J.S. Ali, A. Andleeb, H. Butt, M. Zia, A. Mehmood, M. Nadeem, S. Drouet, J.P. Blondeau, Comparative evaluation of chemically and green synthesized zinc oxide nanoparticles: their in vitro antioxidant, antimicrobial, cytotoxic and anticancer potential towards HepG2 cell line. J. Nanostruct. Chem. **13**(2), 243–261 (2023)